Sekyere *et al.*
Journal of Electrical Systems and Inf Technol (2024) 11:25
https://doi.org/10.1186/s43067-024-00149-x

Journal of Electrical Systems and Information Technology

RESEARCH Open Access

Optimally tuned cascaded FOPI-FOPIDN with improved PSO for load frequency control in interconnected power systems with RES

Yaw O. M. Sekyere[1*], Francis B. Effah[1] and Philip Y. Okyere[1]

*Correspondence: yawsekyere@gmail.com

[1] Electrical Engineering Department, Kwame Nkrumah University of Science and Technology, Kumasi, Ghana

Abstract

In the operation and control of power systems, load frequency control (LFC) plays a critical role in ensuring the stability and reliability of interconnected power systems. Modern power systems with significant penetration of highly variable and intermittent renewable sources present new challenges that make traditional control strategies ineffective. To address these new challenges, this paper proposes a novel LFC strategy that employs a cascaded fractional-order proportional integral-fractional-order proportional integral derivative with a derivative filter (FOPI-FOPIDN) as a controller. The parameters of the FOPI-FOPIDN are optimised using a variant of the particle swarm optimization (PSO) in the literature called ADIWACO. The effectiveness and scalability of the proposed strategy are validated by extensive simulations conducted on two- and three-area test systems and performance comparisons with recent LFC control strategies in the literature. The performance metrics used for the evaluation are ITAE values, deviations in the power flows in the tie-lines, and deviations in the frequencies of the control areas with the power systems subjected to diverse load and RES generation disturbances in several experimental scenarios. Governor dead band, communication time delay, and generation rate constraints are considered in one of the scenarios for more realistic evaluation. Again, the controller's robustness to uncertain model parameters is validated by varying the parameters of the three-area test system by ± 50%. The simulation results obtained confirm the controller's robustness and its superiority over the comparison LFC strategies in terms of the above performance metrics.

Keywords: Load frequency control (LFC), Automatic generation control (AGC), Particle swarm optimization application, Fractional order controllers, Renewable energy sources (RES), Power systems

Background

An interconnected power system comprises several control areas connected by tie lines to exchange power among them. The load in power systems is never steady, it continually changes with rising and falling trends. Failing to match any small sudden load change in any control area in an interconnected power system will change the system frequency and power flows in the tie lines. Large deviations in frequency can lead to power system instability and large fluctuations in tie-line power flows. Therefore, it is important in an

© The Author(s) 2024. **Open Access** This article is licensed under a Creative Commons Attribution 4.0 International License, which permits use, sharing, adaptation, distribution and reproduction in any medium or format, as long as you give appropriate credit to the original author(s) and the source, provide a link to the Creative Commons licence, and indicate if changes were made. The images or other third party material in this article are included in the article's Creative Commons licence, unless indicated otherwise in a credit line to the material. If material is not included in the article's Creative Commons licence and your intended use is not permitted by statutory regulation or exceeds the permitted use, you will need to obtain permission directly from the copyright holder. To view a copy of this licence, visit http://creativecommons.org/licenses/by/4.0/.

interconnected power system to maintain an active power balance in all control areas to keep the system frequency and the tie-line power flows as close as possible to their scheduled values. In a large power interconnected system, the load is matched at the control area level by regulating the active power produced by generators in the control area using load frequency control (LFC). The balance in a control area is reached when the scheduled power exchange with neighbouring control areas equals the actual power exchange. In the presence of continually varying load, balancing active power between generation and load is a very challenging task, requiring superior controllers for the load frequency control. Widely used controllers are the Proportional-Integral (PI), and Proportional-Integral-Derivative (PID) controllers because of their simple structure [1–3]. There are several traditional and modern methods for tuning these controllers to get the best performance out of them.

The integration of renewable energy sources (RES) into conventional power systems has become a defining imperative in the quest for sustainable and environmentally responsible energy generation [4, 5]. As the global community strives to reduce carbon emissions and transition towards cleaner energy sources, RES such as wind and solar have gained widespread attention for their potential to reshape the power generation landscape. However, integrating renewable energy sources into the power grid presents significant challenges [6–8]. Due to their intermittency and randomness, renewable energy sources complicate the balancing of active power between generation and load. This increased complexity necessitates the use of more advanced controllers for load frequency control [9, 10].

Literature review

Several different methods have been proposed in the literature to achieve more efficient LFC strategy capable of maintaining active power balance between generation and load in the presence of severe power system disturbances. These methods include state estimation techniques like Kalman filtering [1], Extended and Unscented Kalman Filter [11], data-driven modeling and system identification approaches [6], reinforcement learning-based control [12–15], fuzzy logic control for rule-based adaptability [1, 16–18], and signal processing methods such as the wavelet transform [19]. Among these diverse methodologies, H-infinity (H∞) control stands out as a control theory approach that seeks to design controllers to minimize the worst-case effects of uncertainty and disturbances in a system [20–22]. The H∞ control has proved to play a crucial role in achieving robust and optimal regulation of the power system's frequency and tie-line power flow while accounting for uncertainties and disturbances [20–24]. Model predictive control (MPC) is another advanced control strategy that offers a predictive approach to control, allowing for real-time optimization of control actions based on predictions of system behavior [23–25]. However, these proposed methods in the literature to increase the control quality of RES-integrated power systems exhibit various limitations. Kalman filtering, while effective, can be computationally intensive [10, 26, 27]. Advanced state estimation techniques, such as the Extended Kalman Filter and Unscented Kalman Filter [11], can be computationally demanding, making real-time implementation challenging. Fuzzy logic control relies on expert knowledge and rule-based systems, potentially making it less adaptable to unforeseen changes

[28, 29]. H-Infinity control is generally complex to implement and necessitates a clear understanding of system uncertainties and performance specifications. MPC comes with computational intensity, potential latency, complex implementation, and sensitivity to modelling errors [23, 30, 31].

In response to the challenges and computational demands posed by these advanced control strategies in load frequency control, researchers are actively focusing on the use of fixed gain controllers. The design method of this type of controller is a two-step procedure consisting of determining the controller structure and finding a suitable method to calculate its parameters. In this controller design approach, researchers are actively exploring the use of metaheuristic optimization techniques to obtain the optimal gain parameters for the fixed gain controllers. This pursuit extends to traditional controllers such as Proportional-Integral (PI) [32] and Proportional-Integral-Derivative (PID) [33, 34], along with innovative controller structures like the cascaded Tilt Integral Derivative–PID (TID-PID) tuned by Grey Wolf Optimization (GWO) algorithm [35] and Teaching Learning-Based Optimization (TLBO) algorithm [36]. The literature presents a diverse array of controller designs, including the introduction of a firefly-optimized fuzzy PID controller [37], the application of the Flower Pollination algorithm for gain parameter optimization in a cascaded PI-PD controller [38], and the optimal tuning of a PID controller with derivative noise filters (PIDN) using Particle Swarm Optimization (PSO) algorithm [39]. In 2018, Genetic Algorithm (GA) was employed to optimally tune a cascaded PD-PID controller with double derivative filters (PDPID plus DDF) [40]. In 2021, improved frequency deviation results were achieved with this same structure by employing the Symbiotic Organism Search (SOS) algorithm to tune it [41].

The traditional controllers optimized for a specified operating condition may sometimes not work efficiently where operating conditions change with continuously varying load demands [33] and high penetration of RES. Hence, fractional order controllers are gaining the attention of researchers to enhance further the efficacy of LFC. Fractional order controllers introduce greater flexibility through the incorporation of fractional order derivative and integral terms [42]. Studies have shown that they provide better performance in various power system structures [42]. In related works, Lion Algorithm optimized fractional order proportional integral (FOPI) controller was applied in a two-area power system in [43]. FOPID has also been used in a number of studies for LFC tuned with different metaheuristics like the Big Bang Big Crunch (BBBC) optimization algorithm [44], Bacteria Foraging Technique (BFT) [45], and a hybrid Genetic Algorithm-Firefly Algorithm (hGA-FA) [46]. Several different cost functions like the integral time absolute error (ITAE) [46], integral time square error (ITSE) [47], integral square error (ISE) [45], and integral absolute error (IAE) [44] have been used. More sophisticated cascaded fractional order controllers in the literature include FOPI-FOIDN optimally tuned by Crow Search Algorithm (CSA) [48], PIDN-FOID optimized by the Whale Optimization Technique (WOT) [49], WOT tuned IDN-FOPD controller [50], PIFOD-(1 + PI) tuned by Yellow Saddle Goatfish Algorithm (YSGA) [51] and FOPI-FOPD tuned by Sine Cosine Algorithm (SCA) [52].

Research gap and challenges

The presence of high-frequency noise introduces a vulnerability in fractional order controllers with derivatives, for example, when used for hydropower [42]. In response to this challenge, researchers have predominantly favoured the utilization of Fractional Order Proportional-Integral (FOPI) [43, 53] and Integral (FOI) controllers [6] particularly for hydro plants, while fractional order derivative controllers have predominantly found applications in the secondary control for thermal plants in the literature [49–53]. The FOPI and FOI controllers, which do not incorporate fractional order derivatives, may exhibit slightly more oscillations around the desired frequency as compared to fractional order controllers with derivative action included [42]. In an attempt to use fractional order controllers with derivative action on hydro plants, fuzzy logic controllers have been cascaded with ICA-tuned FOPI-FOPID in the study reported in [54] and PIDN-FOPIDN reported in [55]. The main drawback of fuzzy logic controllers in load frequency control is their inherent difficulty in precisely capturing and modeling complex nonlinear system dynamics [54, 56].

Contribution

To address the above challenges more effectively, this paper includes an optimized derivative filter in the FOPI-FOPID structure to obtain FOPI-FOPIDN for a control area, which contains hydro and thermal plants, as well as renewable energy sources (RES). The gain parameters of the proposed controller consisting of fractional order parameters, and the filter coefficient "N" are then optimized using a PSO variant, which like the standard PSO, has few parameters to tune and is easy to program. The PSO variant called ADIWACO, developed by the authors, combines adaptive and dynamic techniques to adjust the inertia weight and acceleration coefficients of the standard PSO (SPSO) [57]. ADIWACO has proved to be effective in tuning traditional PID controllers for load frequency control of interconnected power systems with RES [58].

Paper organization

The rest of the paper is structured as follows: "Test systems" section provides a detailed description of the test systems utilized in this study. In "FOPIFOPIDN controller" section, the proposed FOPI-FOPIDN controller is presented. "Improved PSO (ADIWACO)" section gives an overview of the PSO variant, ADIWACO, used to optimally tune the FOPI-FOPIDN controller. "Implementation" section presents the simulation results, accompanied by discussions highlighting the efficacy of the proposed methodology. Finally, "Optimal tuning of the controllers" section concludes the paper with a summary of key findings, implications, and avenues for future research.

Test systems

Two widely used test systems depicted in Figs. 1 and 2 are considered. Their comprehensive details are available in [6, 19, 34–36, 54, 55, 59, 60]. Test system 1 represents a two-area power system having thermal reheater and hydro plants as conventional

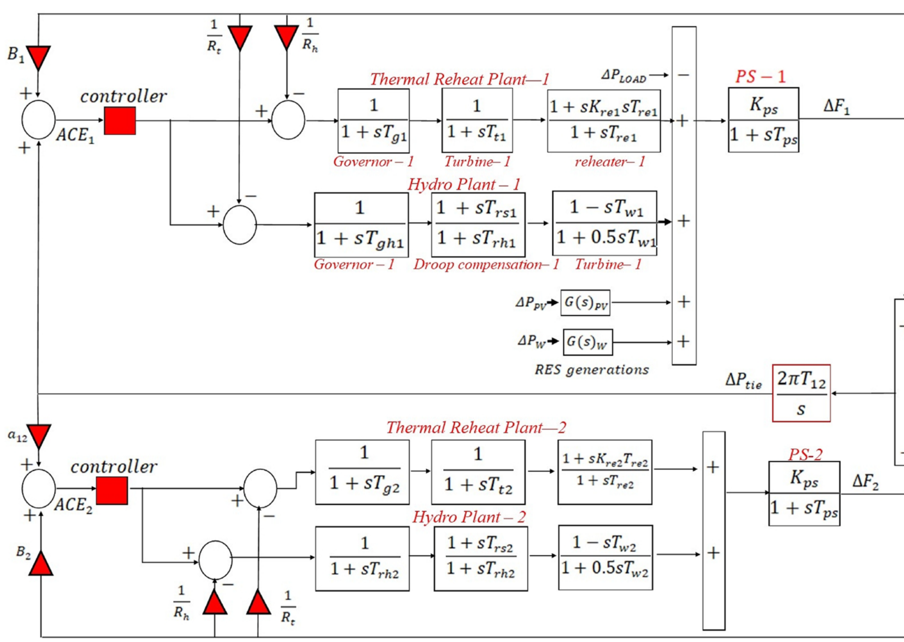

Fig. 1 Test system 1

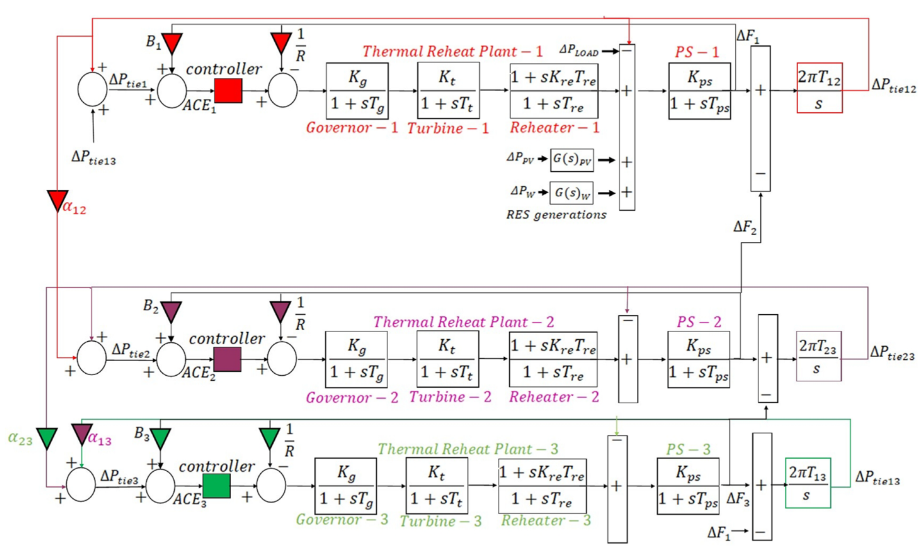

Fig. 2 Test system 2

sources in each area. In addition, wind and solar units are connected in area 1. The second test system, which is a three-area power system, is used to verify the scalability of the proposed LFC strategy. This power system has a thermal reheater plant in each control area, representing all conventional coherent generators within the control area. Additionally, wind and solar units are integrated in Area 1.

The transfer functions for the wind turbine plant, $G(s)_{WTG}$, and solar PV plant, $G(s)_{PV}$, given in Figs. 1 and 2, are defined as follows [6]:

$$G(s)_{WTG} = \frac{K_{wTG}}{1 + sT_{wTG}} \tag{1}$$

$$G(s)_{PV} = \frac{K_{PV}}{1 + sT_{PV}} \tag{2}$$

where K_{WTG} and K_{PV} are the respective gains of the wind turbine and solar PV plants and T_{WTG} and T_{PV} are their respective time constants.

FOPIFOPIDN controller

The proposed load frequency control strategy is based on a fractional-order Proportional Integral cascaded with a fractional-order Proportional Integral Derivative with a derivative filter (FOPI-FOPIDN). The structural representation of the cascaded controller is shown in Fig. 3.

The FOPI serves as the master control, addressing tie-line power and frequency deviations using fractional-order calculus [7]. Its parameter λ_1 represents the non-integer order of the integrator and K_{P1} and K_{I1} are the gains of the proportional and integral terms. The output of the FOPI controller is sent to the FOPIDN controller for further fine-tuning and enhanced disturbance rejection. Its parameters λ_2 and μ denote the non-integer order of the integrator and differentiator, respectively, while N represents the derivative filter coefficient. The parameters K_{P2}, K_{I2} and K_D are the gains of the proportional, integral and the derivative terms. The complete transfer function of the cascaded FOPI-FOPIDN system is as follows:

$$C(s)_{FOPI-FOPIDN} = \left(K_{P1} + \frac{K_{I1}}{s^{\lambda 1}}\right)\left(K_{P2} + \frac{K_{I2}}{s^{\lambda 2}} + \frac{NK_D s^{\mu}}{s^{\mu} + N}\right) \tag{3}$$

The main contribution of this methodology is the inclusion of the derivative filter to alleviate the impact of high-frequency noise. The challenge of tuning the filter coefficient to strike a balance between noise attenuation and control responsiveness is effectively addressed through the application of a suitable metaheuristic algorithm. The primary objective of the load frequency control is to maintain a zero Area Control Error (ACE). It is given by (4) for the two-area power system and by (5) for the three-area power system [54].

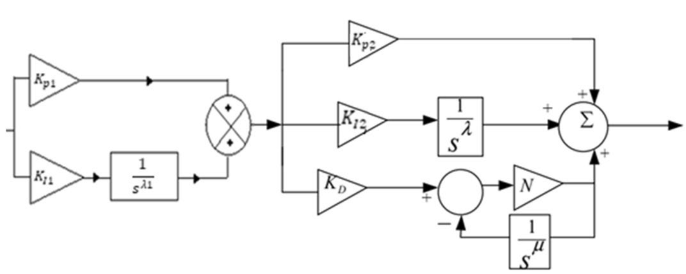

Fig. 3 Structure of the FOPI-FOPIDN cascaded controller

$$\begin{cases} ACE_1 = B_1\Delta F_1 + \Delta P_{tie} \\ ACE_2 = B_2\Delta F_2 + \alpha_{12}\Delta P_{tie} \end{cases} \tag{4}$$

$$\begin{cases} ACE_1 = B_1\Delta F_1 + \Delta P_{tie,1} \\ ACE_2 = B_2\Delta F_2 + \Delta P_{tie,2} \\ ACE_3 = B_3\Delta F_3 + \Delta P_{tie,3} \end{cases} \tag{5}$$

and [54]

$$\begin{cases} \Delta P_{tie,1} = \Delta P_{tie,12} + \Delta P_{tie,13} \\ \Delta P_{tie,2} = \alpha_{12}\Delta P_{tie,12} + \Delta P_{tie,23} \\ \Delta P_{tie,3} = \alpha_{13}\Delta P_{tie,13} + \alpha_{23}\Delta P_{tie23} \end{cases} \tag{6}$$

where B_i is the bias coefficient of control area *i*, ΔF_i is the change in frequency of control area *i* and $\Delta P_{tie,ij}$, is the change in tie-line power transported from control area *i* to control area *j*, α_{ij} is the area rating ratio of control area *i* to control area *j*.

To achieve the primary objective of the LFC, it will be necessary to find the optimal parameters of the FOPI-FOPIDN controller. This task becomes increasingly complex as the number of controllers needed increases with the number of control areas. This challenge is addressed in this study using the PSO variant called ADIWACO in [57]. The integral time-absolute error (ITAE) given by (7) for the two-area power system and by (8) for the three-area power system is used as its fitness functions [34, 54].

$$J_{sys,1} = \int_0^T \left[|\Delta f_1| + |\Delta f_2| + |\Delta P_{tie,1}| \right] tdt \tag{7}$$

$$J_{sys,2} = \int_0^T \left[|\Delta f_1| + |\Delta f_2| + |\Delta f_3| + |\Delta P_{tie,1}| + |\Delta P_{tie,2}| + |\Delta P_{tie,3}| \right] tdt \tag{8}$$

where Δf_i represents the change in frequency of control area *i* and $\Delta P_{tie,i}$ the change in the total tie line power transported from control area *i*.

The parameters to be optimally determined for each controller are K_{p1}, K_{p2}, K_{I1}, K_{I2}, K_D, N, λ_1, λ_2 and μ. These parameters are determined subject to the constraints given by (9) from [61]. One controller is required for each control area of a power system.

$$setconstraints \begin{cases} 0 < K_P < 10 \\ 0 < K_I < 20 \\ 0 < K_D < 5 \\ 0 < \mu < 2 \\ 0 < \lambda < 2 \end{cases} \tag{9}$$

Improved PSO (ADIWACO) [56]

The standard PSO is a swarm-based optimization technique inspired by the collective behavior of bird flocks or fish schools. In the PSO, a population of potential solutions, represented as particles, explores the solution space by adjusting their positions based on their own best-known solutions and the globally best solution found by the entire population [62]. Mathematically, velocity, *v* and position, *x* of each particle are updated iteratively using the following equations [62]:

$$v_i(t+1) = wv_i(t) + c_1(p_i(t) - x_i(t)) \tag{10}$$

$$x_i(t+1) = x_i(t) + v_i(t+1) + c_2\left(g(t) - x_i(t)\right) \tag{11}$$

where $w =$ the inertia weight $c_1, c_2 =$ acceleration coefficients, $x_i(t)$=the current position of a particle, $x_i(t+1)$=the updated position of a particle, $p_i(t)$=the personal best of a particle, $g(t)$=the global best of a particle,$v_i(t)$=the velocity of a particle and $v_i(t+1)$=updated velocity of the updated particle with the position $x_i(t+1)$ [62].

The standard PSO uses constant inertia weight and acceleration coefficients [63]. The improved PSO in [57] enhances its performance by employing adaptive dynamic inertia weight and acceleration coefficients. The inertia weight, w is defined as follows:

$$w = \mu \tanh \delta \tag{12}$$

where

$$\mu = \frac{Personal_{best} - Global_{best}}{Personal_{best}} \tag{13}$$

$$\delta = W_{max} - \frac{(W_{max} - W_{min}) \times the\ number\ of\ the\ current\ iteration}{Maximum\ number\ of\ iterations} \tag{14}$$

where W_{max} and W_{min} represent the upper and lower limits of the inertia weight respectively. The parameter μ lies in the range [0, 1]. The acceleration coefficients are calculated at each iteration as follows:

$$c_1 = c_2 = \mu \cosh \psi \tag{15}$$

where

$$\psi = C_{max} - \frac{(C_{max} - C_{min}) \times the\ number\ of\ the\ current\ iteration}{Maximum\ number\ of\ iterations} \tag{16}$$

Tuning algorithm

The ADIWACO PSO is used as follows to obtain the optimal values of K_{p1}, K_{p2}, K_{I1}, K_{I2}, K_D, N, λ_1, λ_2 and μ for each of the cascaded fractional order controllers (FOPI-FOPIDN).

Step 1: Model the test system in MATLAB/Simulink.

Step 2: Initialize the following PSO parameters: population size, dimension of particle, maximum number of iterations, minimum and maximum inertial weights, and minimum and maximum acceleration coefficients. Set initial personal and global best as infinity.

Step 3: Generate initial random population of particles with dimension D, each particle representing the gains of all the controllers.

Step 4: Introduce a step load perturbation and run the simulation.

Step 5: While iteration < maximum number of iterations **do**

Calculate ITAE of each particle using (7) or (8) for a specified T

If particle ITAE < particle best **then**

particle best **=** particle ITAE

If particle best < global best **then**

global best = particle best

end if

end if

Update particle velocities and positions using (10) and (11) respectively

Step 6: Set the global best particle as the FOPI-FOPIDN controller parameters

Implementation

The performance of the proposed LFC strategy is evaluated on the test systems presented in Figs. 1 and 2 using MATLAB / Simulink Software (R2023a). The computer setup used for the testing has the following specifications: Windows 11 (64-bit) for the software environment and an Intel(R) Core (TM) i5-8250U CPU @ 1.60 GHz 1.80 GHz with 24.0 GB installed RAM for the hardware environment. The parameters of the two-area and the three-area power systems are presented in the "Appendix" section.

Optimal tuning of the controllers

The parameters of the PSO variant (ADIWACO) are presented in the "Appendix" section. For successful implementation of the algorithm, a maximum number of iterations of 100, commonly used in the literature for metaheuristic algorithms for this type of application, is chosen. The tuning was done using a step load perturbation of 0.1 pu in area 1 of the power systems. The convergence rate curve given in Fig. 4 shows that the algorithm converged in fewer than 30 iterations for both test systems and that the maximum iterations of 100 was more than it was required.

Testing

The effectiveness of the LFC strategy using FOPI-FOPIDN controllers is assessed on both test systems, employing optimal parameters obtained through the ADIWACO algorithm. The assessment is done using step load perturbation, combined random load, PV and wind perturbations, and system parameters variation. The resulting ITAE values, frequency, and tie-line power responses are compared with those of various strategies

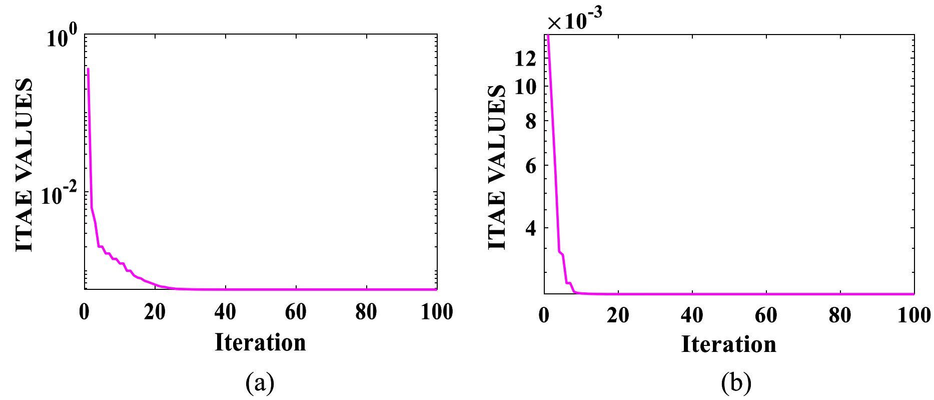

Fig. 4 Convergence profile of proposed algorithm for **a** test system 1 and **b** test system 2 with FOPI-FOPIDN controller

Table 1 Optimal gain parameters obtained

Gain parameters	Two area	Three area	Three area tuned with physical constraints included
K_{p1}	4.6121	5.3898	0.1
K_{I1}	14.285	20	0.1
λ_1	0.90464	0.95363	0.1
K_{p2}	3.5608	10	1.7535
K_{I2}	17.292	20	0.3797
λ_2	0.1	0.1	0.1
K_D	1.141	1.8457	1.764
μ	1.3147	1.3283	1.3186
N	351.63	500	289.57

from the literature to establish its superiority. Models of the test systems, with and without physical constraints, are considered. The parameters obtained for the FOPI-FOPIDN controllers deemed to be identical during tuning are presented in Table 1.

On the test system 1, widely used in the literature to test PID controllers, the performance of the proposed FOPI-FOPIDN controllers is benchmarked against PID controllers with gain parameters determined by ADIWACO [58], Magnetotactic Bacteria Optimizer (MBO) [6], Grey Wolf Algorithm [34], and a hybrid Firefly Algorithm and Pattern Search Technique [64]. Additionally, it is compared with cascaded fuzzy PID-fractional-order PID with double derivative filters (FPIDN-FOPIDN), tuned by the Imperialist Competitive Algorithm (ICA) [59].

Similarly, on test system 2, the comparison controllers are PID tuned by ADIWACO [58], FPIDN-FOPIDN tuned by ICA [59], Cascaded Fuzzy FOPI–FOPID tuned by ICA [54], Fuzzy FOPI–FOIDN tuned by Crow Search Algorithm (CSA) [65], and FOPI–FOPID with no derivative filter tuned by ADIWACO.

Results and discussion

Models without physical constraints

Test Systems 1 and 2 are employed for various experimental scenarios.

Step load perturbation: test system 1

An incremental step load perturbation of 0.1 pu is applied in area 1 of Test System 1 as the sole disturbance. The responses of area one frequency, area two frequency, and tie line power flow for the six LFC strategies are compared in Figs. 5, 6 and 7, and ITAE values in Table 2. From the curves, the LFC strategy based on the proposed ADIWACO-tuned FOPI-FOPIDN controllers outperforms all the variously tuned PID controllers and the cascaded fuzzy PID-fractional-order PID with double derivative filters (FPIDN-FOPIDN) in terms of deviations in all the responses and thus yielding the best overshoot, undershoot and settling time. The steady-state errors are zero for all. In terms of the ITAE values, the ADIWACO-tuned FOPI-FOPIDN controller shows 10.7826% improvement on ICA-tuned FPIDN-FOPIDN, 30.96% on ADIWACO tuned PID, 96.29% on hFA-PS tuned PID, 96.3797% on GWO tuned PID and 99.99% on MBO tuned PID controllers. This confirms the superior performance of

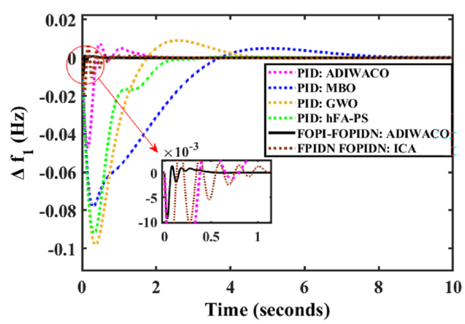

Fig. 5 Area 1 change in frequency, test system 1, SLP = 10%

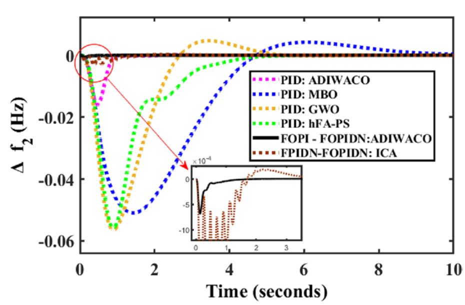

Fig. 6 Area 2 change in frequency, test system 1

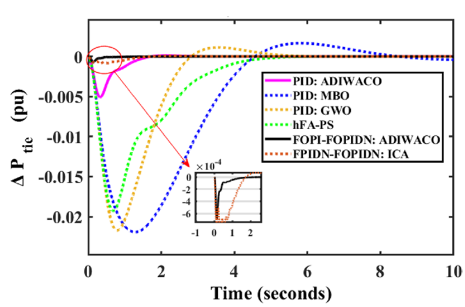

Fig. 7 Change in tie line power, test system 1

Table 2 ITAE values for step perturbation—test system 1 (sampling time = 10 s)

LFC strategy	ITAE value
Proposed FOPI-FOPIDN:ADIWACO	0.01026
PID: ADIWACO [58]	0.01486
PID: MBO [6]	187.00
PID: GWO [34]	0.2834
PID: hFA-PS [64]	0.2764
FPIDN-FOPIDN:ICA [59]	0.0115

the proposed FOPI-FOPIDN-based LFC over the other LFC strategies in mitigating the impact of step load perturbations.

Step load perturbation: test system 2

The same incremental step load perturbation of 0.1 pu is applied in area 1 of the Test System 2. The responses of the area frequencies and the tie-line power flows for the six LFC strategies are compared in Figs. 8, 9, 10, 11, 12, 13 and 14. Their ITAE values are presented in Table 3. In this scenario also, the curves clearly show that the proposed LFC strategy gives the least settling time, overshoot and undershoot in the responses of the tie-line power flows and frequencies. The proposed strategy also demonstrates remarkable performance improvements over the comparison LFC strategies in terms of the ITAE values. Specifically, it shows 92.6864% improvement on the ICA tuned FFOPI-FOPID, 99.0593% over the ICA tuned FPIDN-FOPIDN and 99.7628% on ADIWACO tuned PID. The highest improvement, representing 99.9986%, is obtained over that of a recent CSA-tuned FFOPI-FOIDN. The least improvement of 74.4848% is obtained over

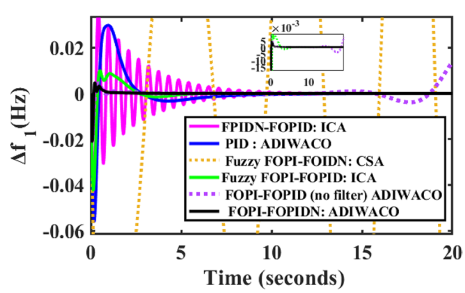

Fig. 8 Area 1 change in frequency for test system 2

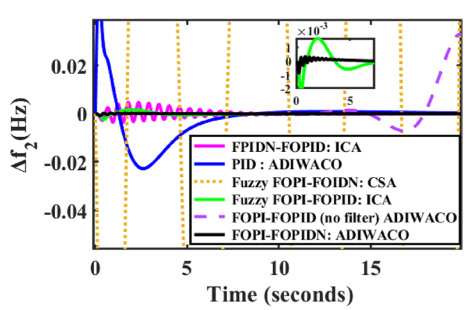

Fig. 9 Area 2 change in frequency for test system 2

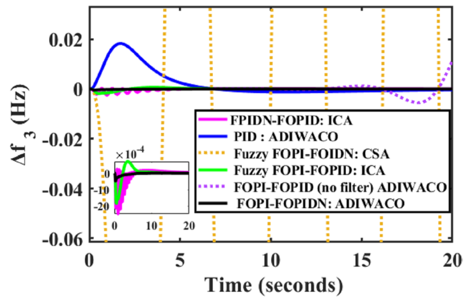

Fig. 10 Area 3 change in frequency for test system 2

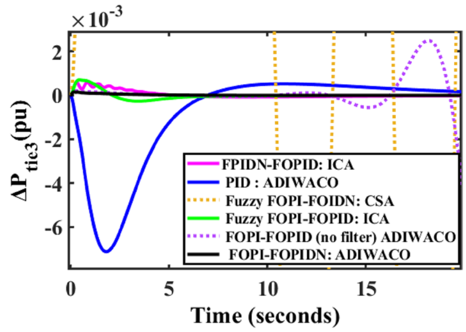

Fig. 11 Area 1 change in tie line power for test system

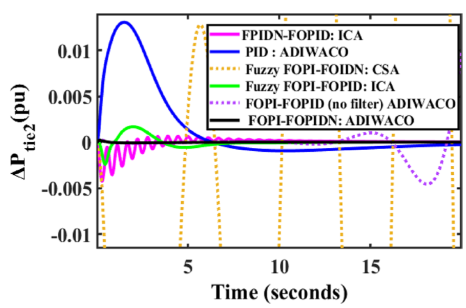

Fig. 12 Area 2 change in tie line power for test system 2

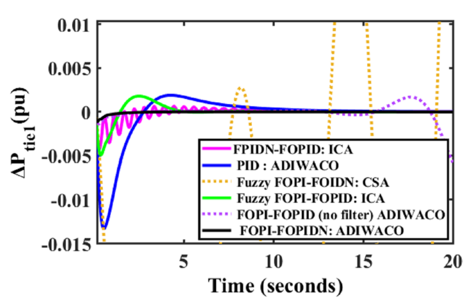

Fig. 13 Area 3 change in tie line power for test system 2

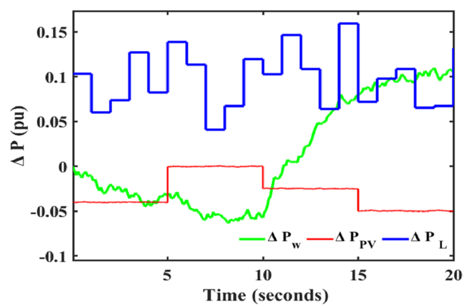

Fig. 14 RLP and changes in solar and wind generations

Table 3 ITAE values for step perturbation—test system 2 (sampling time = 20 s)

LFC strategy	ITAE value
Proposed FOPI-FOPIDN:ADIWACO	0.0026
PID: ADIWACO [58]	1.096
FFOPI-FOIDN:CSA [59]	187.00
FFOPI-FOPID:ICA [54]	0.03555
FPIDN-FOPIDN:ICA [65]	0.2764
FOPI-FOPID (No derivative filter):ADIWACO	0.01019

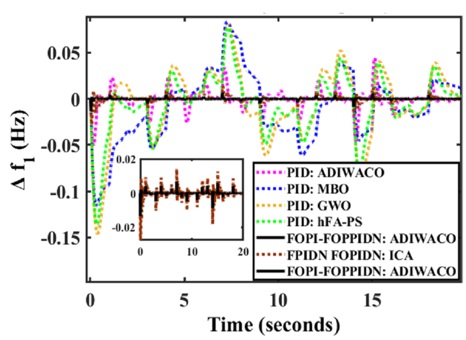

Fig. 15 Scenario 2 Δf_1 for test system 1

that of ADIWACO-tuned FOPI-FOPID with no derivative filters. These results reaffirm the superiority of the proposed FOPI-FOPIDN-based LFC strategy over the comparison controller in mitigating the impact of step load perturbations.

Renewable energy source integration: test system 1

A random load perturbation combined with wind and solar generation perturbations as in [29] is applied to area 1 of Test System 1. The three perturbations are shown in Fig. 14. This scenario is used to verify the performance of the controllers in the presence of random load and variable renewable energy sources. The simulation results for the proposed LFC strategy and the comparison LFC strategies are presented in Figs. 15, 16 and 17. Additionally, Table 4 provides the corresponding ITAE values. The proposed LFC strategy gives the least deviations in all the responses. This is

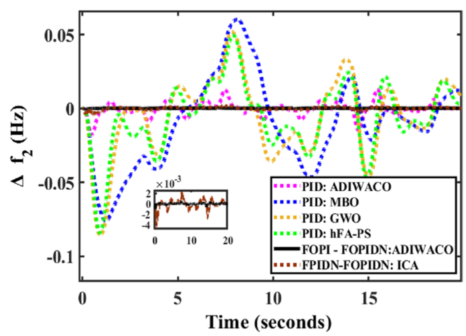

Fig. 16 Scenario 2 Δf_2 for test system 1

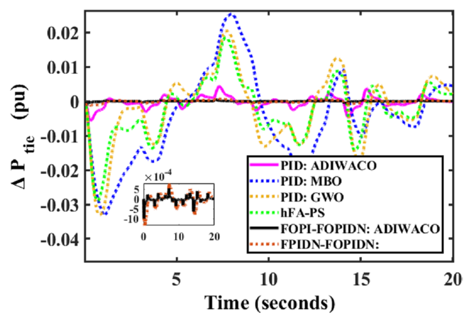

Fig. 17 Scenario 2 ΔP_{tie} for test system 1

Table 4 ITAE values for renewable source integration—test system 1 (sampling time = 20 s)

LFC strategy	ITAE
Proposed FOPIFOPIDN:ADIWACO	0.01026
PID: ADIWACO [58]	0.01486
PID: MBO [6]	187.00
PID: GWO [34]	0.2834
PID: hFA-PS [64]	0.2764
FPIDN-FOPIDN:ICA [59]	0.0115

confirmed by its ITAE value which is the least closely followed by ICA tuned FPIDN-FOPIDN. The results clearly indicate its robustness in the presence of severe power disturbance.

Renewable energy source integration: test system 2

The disturbance in Fig. 14 is also applied in area 1 of Test System 2. The relevant responses are presented in Figs. 18, 19, 20, 21, 22 and 23 and the ITAE values in Table 5. Consistent with the previous results, the proposed LFC strategy demonstrates the least deviations in all responses and the lowest ITAE value. This reaffirms its superior performance when subjected to severe power disturbances and highlights its potential application to larger interconnected power systems.

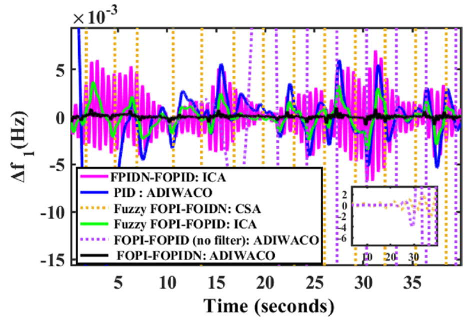

Fig. 18 Area 1 change in frequency for test system 2

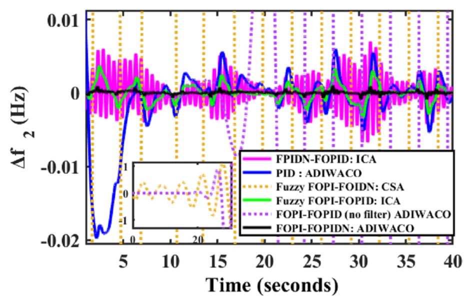

Fig. 19 Area 2 change in frequency for test system 2

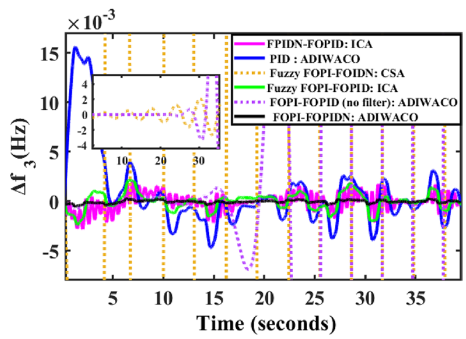

Fig. 20 Area 3 change in frequency for test system 2

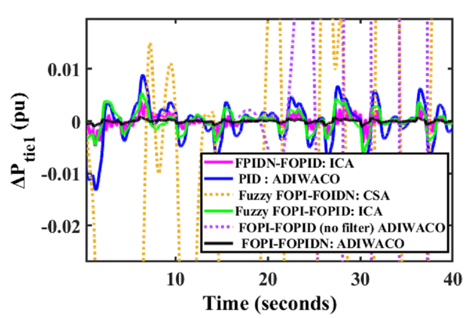

Fig. 21 Area 1 change in tie line power for test system 2

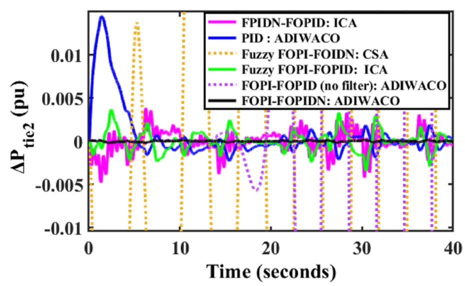

Fig. 22 Area 2 change in tie line power for test system 2

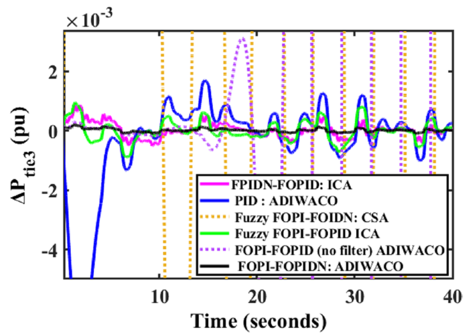

Fig. 23 Area 3 change in tie line power for test system 2

Table 5 ITAE values for renewable source integration—test system 2 (sampling time = 40 s)

LFC strategy	ITAE value
Proposed FOPI-FOPIDN:ADIWACO	1.581
PID: ADIWACO [58]	14.79
FFOPI-FOIDN:CSA [59]	2200.000
FFOPI-FOPID:ICA [54]	7.773
FPIDN-FOPIDN:ICA [65]	11.400
FOPI-FOPID (no derivative filter):ADIWACO	120,800

System parameters variation

To further assess the robustness of the strategy under uncertain system model parameters, the parameters of the Test System 1: K_{ps}, T_{ps}, T_t, T_p, T_g and R are varied by ± 50% as in [60]. Figures 24 and 25 present a comparison of the responses of area 1 and area 2 frequencies with the nominal and changed parameter values. As seen from the curves, a change in parameters within ± 50% range will not significantly affect the performance of the controller. This affirms that the controller is robust enough to perform just as predicted by the simulation results even if the parameters used for the system model are within ± 50% of the actual power system parameters.

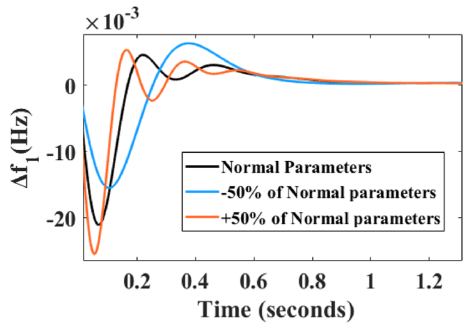

Fig. 24 Area 1 change in frequency

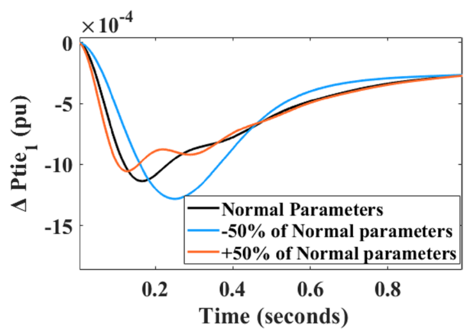

Fig. 25 Area 1 tie line power response

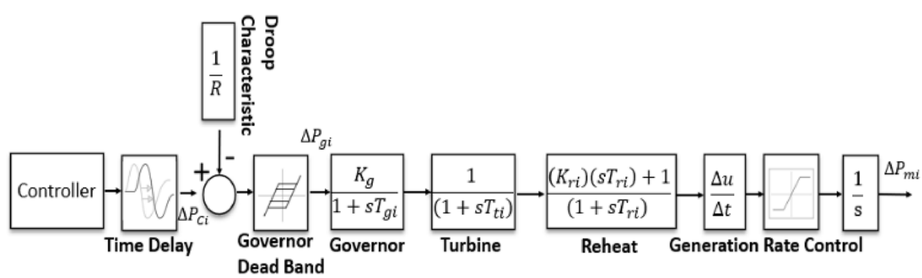

Fig. 26 Block diagram representation of all three constraints [66]

System model of test system 2 with physical constraints included

Regardless of the controller type or the metaheuristic algorithm used in tuning the controller parameters, the LFC system responds more efficiently without physical constraints, showing quicker recovery to the nominal frequency and less deviation during transients [66]. When non-linear physical constraints are imposed, regular controllers may struggle to meet desired performance, taking longer to restore nominal frequency and damping oscillations after external disturbances [66]. To test the efficacy of the proposed LFC strategy on a more practical system, the following physical constraints are considered in the models of the test systems as shown in Fig. 26: communication time delay (TD), generation rate constraints (GRC) and governor dead band (GDB). These constraints are widely adopted in the literature for realistic assessment of the performance of LFC strategies [60, 64, 66–69].

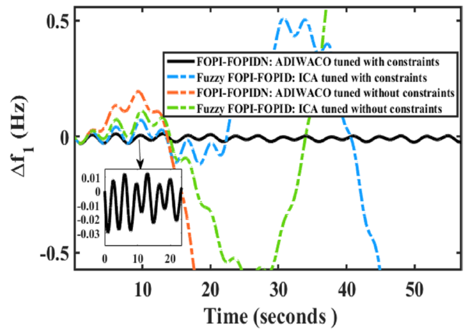

Fig. 27 Effects of incorporating constraints during tuning on area 1 frequency response

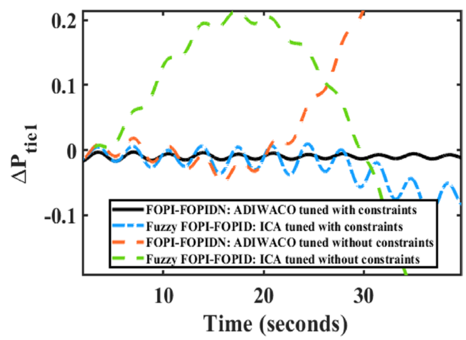

Fig. 28 Effects of incorporating constraints during tuning on Area 1 tie line power response

Including GRC, GDB, and CTD in test system 1

Various studies on Test System 2 use time delays of 5 ms or 10 ms [33] and typical GRC is quoted as 10% pu/min (equivalent to 0.0017 pu/s) for thermal reheater plants in [66]. It is also a common practice to set Governor Dead Band between 15 and 100 mHz across many countries [69, 70]. Therefore, in this study, values of 10% pu/min, 100 mHz, and 10 ms are chosen for GRC, GDB, and CTD respectively. An incremental step load perturbation of 10% is applied in area 1 of the test system. The simulation results obtained are compared with those of the ICA tuned cascaded fuzzy FOPI-FOPID, which has proved to be competitive in terms of ITAE values, in Figs. 27 and 28. Two cases are considered. In one case, the two controllers are tuned with the physical constraints included in the power system model, and in the other case without the physical constraints. From the two figures, the performance of the two controllers is poor when tuning is without constraints. When tuned with the constraints the proposed LFC strategy clearly shows far better performance than the LFC strategy based on the fuzzy FOPI-FOPID. With the fuzzy FOPI-FOPID, both the frequency and tie-line power flow become unstable.

Including GRC, GDB, CTD and RES in test system 2

In this study, power disturbances presented in Fig. 29 are simultaneously applied to in area 1 of Test System 2 with GRC = 10% pu/min, GDB = 100 mHz and CTD = 10 ms. The results presented in Fig. 30 again show that proposed control strategy performs better than the cascaded fuzzy FOPI-FOPID if the controllers are tuned with the constraints

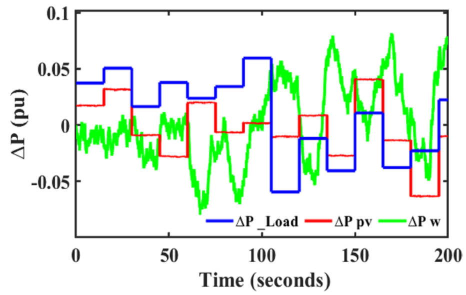

Fig. 29 RLP and changes in solar and wind generations

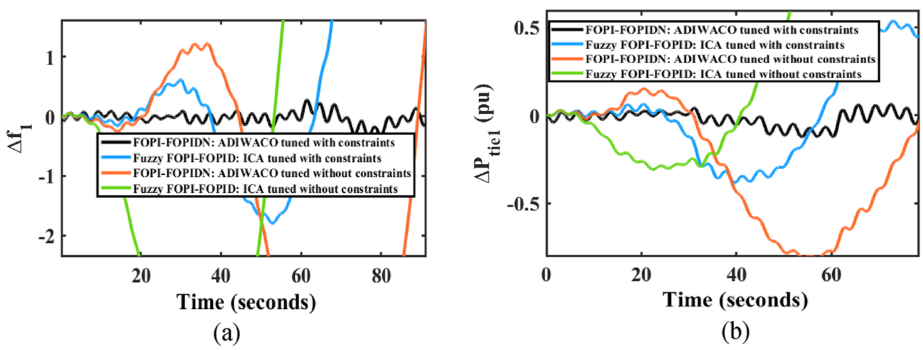

Fig. 30 **a** Δf_1 for RES integration considering physical constraints on test system 2, **b** ΔP_1 for RES integration considering physical constraints on test system 2

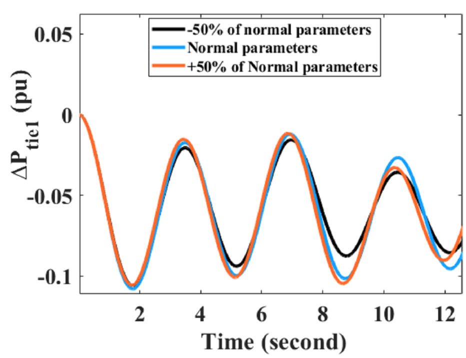

Fig. 31 Effects of System parameters variation on ΔP_{tie1}

included in the test system model. These results confirm the robustness and efficacy of the proposed LFC strategy in the presence of variability and intermittency associated with RES and its potential application to real-world power systems with RES.

Parameter variation with physical constraints, RES integration and random step load perturbation

The results in Figs. 31 and 32 show the responses of Area 1 frequency and tie-line power following simultaneous application of the perturbations in Fig. 14 in Area 1 of Test system 1 for three different parameter settings. GRC, GBD and CTD are included in the test system. The parameter variation has little effect on the tie line power response. In the case of the

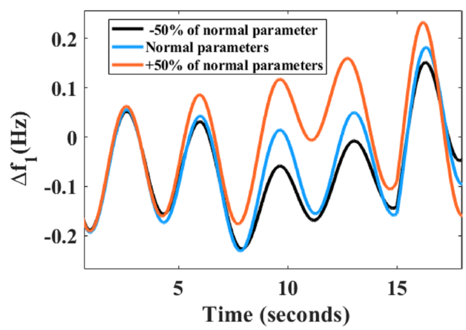

Fig. 32 Effects of system parameters variation on f_1

Area 1 frequency response, the effect of the parameter variation is significant between 8 and 15 s. Outside this period, the effect is negligible. The results show the robustness of the proposed controlling strategy against system parameter variations even when GRC, GBD and CTD are included in the test system.

Conclusion

This paper presents an LFC strategy based on a cascaded fractional-order proportional integral-fractional-order proportional integral derivative (FOPI-FOPIDN) with a derivative filter. The controller is optimally tuned using a PSO variant known as ADIWACO. The robustness and scalability of the proposed LFC strategy are rigorously tested on a two-area test system and then a three-area test system using step load perturbation, and a combined random load, PV, and wind perturbations. The experimental results obtained are compared with those of recent LFC strategies in the literature in terms of ITAE values and deviations in frequencies and tie-line power flows. The results of the comparison analyses clearly show the superiority of the proposed LFC strategy over the comparison LFC strategies. Furthermore, the proposed control strategy is subjected to more stringent testing by incorporating key physical constraints, namely generator rate constraints, governor dead band, and communication time delays in the test system. The robustness of the controller under uncertain system model parameters is also verified through variations in the power system parameters. The simulation results obtained from the above stringent experimental setups and its results indicate the superior performance of the proposed LFC strategy. Overall, the study shows that the proposed LFC strategy is more effective and robust than the recent comparison strategies and has enormous potential for load frequency control in real-world RES-integrated power systems. The limitation of the proposed method is its reliance on fixed gains, which means it is not an adaptive strategy. Future work should explore ways to enhance the adaptiveness of the proposed method.

Appendix

Test system 1

Area 1 rating 2000 MW, Area 2 rating 2000 MW, Area 1 and Area 2 nominal loading 50%, Power System gain, Kps = 100, Power system time constant = 20 s, Droop Constant (1/R) = 0.333 p.u.MW/Hz, Frequency Bias, B_1 = 0.425 p.u.MW/Hz, Synchronization coefficient, $T_{12}=0.545$, Hydro plant governor time constant, $T_{gh}=48.7$ s, Governor reset time, $T_{rs}=5$, Main servomotor time constant, $T_{rh}=0.513$ s, Water start time, $T_w=1$ s, $\alpha_{12}=-1$, Thermal plant governor time constant, $T_g=0.08$ s, Thermal plant turbine time constant, $T_t=0.3$ s. Solar PV generation rating = 500 MW, Solar PV generation participation factor: 0.25, Solar PV time constant, $T_{PV}=1.8$ s, Solar PV gain, $K_{PV}=1$, Wind Turbine generation rating = 500 MW, Wind Turbine generation participation factor 0.25, Wind generation time constant, $T_{WTG}=1.5$ s, Wind turbine generation gain, $K_{WTG}=1$. Area 1 thermal and hydro plants participation factor 0.25 each. Area 2 thermal plant and hydro plant participation factor 0.5 each.

Test system 2

Area 1 rating = 2000 MW, Area 2 rating = 5000 Mw, Area 3 rating = 8000 MW, $\alpha_{12}=-2/5, \alpha_{13}=-2/8, \alpha_{23}=-5/8$, Solar PV generation participation factor 0.33, Wind generation participation factor 0.33, Thermal plant participation factor 0.33. Solar PV generation rating = 500 MW, Solar PV time constant, $T_{PV}=1.8$ s, Solar PV gain, $K_{PV}=1$, Wind Turbine generation rating = 500 MW, Wind Turbine generation participation factor 0.25, Wind generation time constant, $T_{WTG}=1.5$ s, Wind turbine generation gain, $K_{WTG}=1$, Droop Constant (1/R) = 0.417 p.u.MW/Hz, Frequency Bias, / $B=0.425$ p.u.MW/Hz, Synchronization coefficient, $T=0.545$.

PSO parameters

Population size = 20, Dimension, D = 8, Maximum inertia weight $W_{max}=1$, Minimum inertia weight $W_{min}=0.1$, Maximum acceleration coefficient $C_{max}=5$, Minimum acceleration coefficient $C_{min}=2$, Number of iterations = 100.

Abbreviations

LFC	Load frequency control
RES	Renewable energy sources
FOPI-FOPID	Fractional order proportional integral-fractional order proportional integral derivative
N	Derivative filter coefficient
TID	Tilt integral derivative controller
PID	Proportional integral derivative controller
PSO	Particle swarm optimization
ADIWACO	Adaptive dynamic inertia weight acceleration coefficient
GWO	Grey wolf optimization
MBO	Magnetotactic bacteria optimizer
BBBC	Big bang big crunch optimization algorithm
BFT	Bacteria foraging technique
hGA-FA	Hybrid genetic algorithm-firefly algorithm
ITAE	Integral time absolute error
ITSE	Integral time square error
ISE	Integral square error
IAE	Integral absolute error
CSA	Crow search algorithm
WOT	Whale optimization technique
CSA	Sine cosine algorithm
GRC	Generation rate constraint
GDB	Governor dead band
CTD	Communication time delay

Acknowledgements
Not applicable.

Author contributions
We hereby affirm that the collaborative efforts of YOMS, FBE, and PYO were instrumental in the design and implementation of this research. YOMS, FBE, and PYO played key roles in analyzing the results and writing the manuscript. Every named author has thoroughly reviewed and approved of the final manuscript.

Funding
The authors declare that they did not receive any funding for this research.

Availability of data and materials
All data generated or analysed during this study are included in this published article.

Declarations

Competing interests
The authors declare that they have no competing interests.

Received: 12 January 2024 Accepted: 23 June 2024
Published online: 08 July 2024

References
1. Akter K, Nath L, Tanni TA, Surja AS, Iqbal MS (2022) An improved load frequency control strategy for single & multi-area power system. In: 2022 International conference on advancement in electrical and electronic engineering ICAEEE 2022, pp 1–6. https://doi.org/10.1109/ICAEEE54957.2022.9836416
2. Pathik BB, Chowdhury A, Nobi MN, Hasan M, Mahi SA (2022) Automatic load-frequency control using PID controller in an isolated single area and two-area hydro power system. In: ICPC2T 2022—2nd international conference on power, control and computing technologies proceedings. https://doi.org/10.1109/ICPC2T53885.2022.9776813
3. Sahu A, Prasad LB (2018) Load frequency control of interconnected five-area power system with PID controller. In: IEEE international conference on information, communication, instrumentation and control ICICIC 2017, vol 2018, pp 1–8. https://doi.org/10.1109/ICOMICON.2017.8279069
4. Bose U, Chattopadhyay SK, Chakraborty C, Pal B (2019) A novel method of frequency regulation in microgrid. IEEE Trans Ind Appl 55(1):111–121. https://doi.org/10.1109/TIA.2018.2866047
5. Himawan DY, Putranto LM, Setyonegoro MIB, Isnandar S (2021) Maximum penetration of intermittent renewable energy in southern sulawesi system based on primary reserve constrained unit commitment. In: International conference on technology and policy in energy and electric power emerging energy sustainability, smart grid, and microgrid technologies for future power system proceedings, pp 180–185. https://doi.org/10.1109/ICT-PEP53949.2021.9600905
6. Gottapu K, Chennamsetty DP, Isukapalli KK, Gorle PK, Nakka S, Chinta DP (2023) Load frequency control of interconnected power system with renewables using improved fractional integral controller. Int J Renew Energy Res 13(1):392–400. https://doi.org/10.20508/ijrer.v13i1.13561.g8691
7. Yang F et al (2023) Fractional-order sliding mode load frequency control and stability analysis for interconnected power systems with time-varying delay. IEEE Trans Power Syst. https://doi.org/10.1109/TPWRS.2023.3242938
8. Etingov P, Oudalov A, Voropai N, Cherkaoui R, Germond A (2007) Power system stability enhancement using ANN based coordinated emergency control system. In: 2007 IEEE Lausanne POWERTECH, Proceedings, pp 232–237. https://doi.org/10.1109/PCT.2007.4538322
9. Ayamolowo OJ, Manditereza P, Kusakana K (2022) An overview of inertia requirement in modern renewable energy sourced grid: challenges and way forward. J Electr Syst Inf Technol. https://doi.org/10.1186/s43067-022-00053-2
10. Zhang Z, Hu J, Lu J, Cao J, Alsaadi FE (2022) Preventing false data injection attacks in LFC system via the attack-detection evolutionary game model and KF algorithm. IEEE Trans Netw Sci Eng 9(6):4349–4362. https://doi.org/10.1109/TNSE.2022.3199881
11. Wang W, Yorino N, Sasaki Y, Zoka Y, Bedawy A, Kawauchi S (2021) Adaptive model predictive load frequency controller based on unscented Kalman filter. In: Proceedings—2021 IEEE sustainable power energy conference energy transition carbon neutrality, iSPEC 2021, pp 1818–1822. https://doi.org/10.1109/iSPEC53008.2021.9735843
12. Khalid J, Ramli MAM, Khan MS, Hidayat T (2022) Efficient load frequency control of renewable integrated power system: a twin delayed DDPG-based deep reinforcement learning approach. IEEE Access 10(April):51561–51574. https://doi.org/10.1109/ACCESS.2022.3174625
13. Yan Z, Xu Y (2020) A multi-agent deep reinforcement learning method for cooperative load frequency control of a multi-area power system. IEEE Trans Power Syst 35(6):4599–4608. https://doi.org/10.1109/TPWRS.2020.2999890
14. Rozada S, Apostolopoulou D, Alonso E (2020) Load frequency control: a deep multi-agent reinforcement learning approach. IEEE Power Energy Soc Gen Meet. https://doi.org/10.1109/PESGM41954.2020.9281614
15. Liu GX, Liu ZW, Wei GX (2021) Model-free load frequency control based on multi-agent deep reinforcement learning. In: Proceedings of 2021 IEEE international conference on unmanned systems ICUS 2021, pp 815–819. https://doi.org/10.1109/ICUS52573.2021.9641432
16. Chen G, Li Z, Zhang Z, Li S (2020) An improved ACO algorithm optimized fuzzy PID controller for load frequency control in multi area interconnected power systems. IEEE Access 8:6429–6447. https://doi.org/10.1109/ACCESS.2019.2960380
17. Khooban MH, Gheisarnejad M (2021) A novel deep reinforcement learning controller based type-II fuzzy system: frequency regulation in microgrids. IEEE Trans Emerg Top Comput Intell 5(4):689–699. https://doi.org/10.1109/TETCI.2020.2964886

18. Balamurugan CR (2018) Three area power system load frequency control using fuzzy logic controller. Int J Appl Power Eng 7(1):18. https://doi.org/10.11591/ijape.v7.i1.pp18-26
19. Otchere IK, Ampofo DO, Frimpong EA (2017) Adaptive discrete wavelet transform based technique for load frequency control. In: Proceedings of 2017 IEEE PES-IAS PowerAfrica conference on harnessing energy, information and communication technologies afford electricity Africa, PowerAfrica 2017, pp 589–594. https://doi.org/10.1109/PowerAfrica.2017.7991292
20. Horie S, Yukita K, Mathumura T, Goto Y (2017) Load frequency control using H infinity control in case of considering PV. In: 2017 20th International conference on electrical machines and systems ICEMS 2017, pp 1–6. https://doi.org/10.1109/ICEMS.2017.8056445
21. Wu J, Tang X (2022) Distributed robust H-infinity control based on load frequency control of interconnected energy under bounded disturbances. In: 2022 6th International conference on robotics and automation sciences ICRAS 2022, pp 7–11. https://doi.org/10.1109/ICRAS55217.2022.9842028
22. Owen E, Pieper J (2021) The augmented unscented H-infinity transform with H-infinity filtering for effective wind speed estimation in wind turbines. In: 2021 IEEE electrical power and energy conference EPEC 2021, pp 163–170. https://doi.org/10.1109/EPEC52095.2021.9621395
23. Wang F et al (2022) Design of model predictive control weighting factors for PMSM using Gaussian distribution-based particle swarm optimization. IEEE Trans Ind Electron 69(11):10935–10946. https://doi.org/10.1109/TIE.2021.3120441
24. Xu R, Zhang G, Zhang K (2021) Coordinated control of wind farm power prediction based on PSO-MPC model. In: Proc. 2021 IEEE 2nd international conference on information technology, big data and artificial intelligence ICIBA 2021, vol 2, no Iciba, pp 1176–1180. https://doi.org/10.1109/ICIBA52610.2021.9688012
25. Oshnoei A, Kheradmandi M, Khezri R, Mahmoudi A (2021) Robust model predictive control of gate-controlled series capacitor for LFC of power systems. IEEE Trans Ind Inform 17(7):4766–4776. https://doi.org/10.1109/TII.2020.3016992
26. Gautam VV, Loka R, Parimi AM (2022) Analysis of load frequency control using extended Kalman filter and linear quadratic regulator based controller. In: 2022 2nd International conference on power electronics and IoT application in renewable energy and its control PARC 2022, pp 1–5. https://doi.org/10.1109/PARC52418.2022.9726570
27. Beura S, Padhy BP (2023) Implementation of novel reduced-order H∞Filter for simultaneous detection and mitigation of FDI-attacks in AGC systems. IEEE Trans Instrum Meas 72:1–12. https://doi.org/10.1109/TIM.2022.3224996
28. Srinivasa Rao C (2012) Adaptive neuro fuzzy based load frequency control of multi area system under open market scenario. In: IEEE-international conference on advances in engineering, science and management ICAESM-2012, pp 5–10
29. Eshetu W, Sharma P, Sharma C (2018) ANFIS based load frequency control in an isolated micro grid. In: Proceedings of IEEE international conference on industrial technology, vol 2018, pp 1165–1170. https://doi.org/10.1109/ICIT.2018.8352343
30. Raghu N (2013) Model predictive control: history and development. Int J Eng Trends Technol 4(6):2600–2602
31. Mohan AM, Meskin N, Mehrjerdi H (2022) MPC-based virtual inertia control of islanded microgrid load frequency control and DoS attack vulnerability analysis. In: 3rd International conference on smart grid and renewable energy, SGRE 2022—Proceedings, pp 1–6. https://doi.org/10.1109/SGRE53517.2022.9774122
32. Singh J (2016) Load frequency control of two area power system with integral proportional-integral and PID controller. Int J Res Eng Technol 05(07):454–460. https://doi.org/10.15623/ijret.2016.0507070
33. Sekyere YOM, Effah FB, Okyere PY (2024) Optimal tuning of PID controllers for LFC in renewable energy source integrated power systems using an improved PSO. In: Accepted manuscript. JEEE, pp 1–18
34. Guha D, Roy PK, Banerjee S (2016) Load frequency control of interconnected power system using grey Wolf optimization. Swarm Evol Comput 27:97–115. https://doi.org/10.1016/j.swevo.2015.10.004
35. Guha D, Roy PK, Banerjee S (2018) A maiden application of modified grey Wolf algorithm optimized cascade tilt-integral-derivative controller in load frequency control. In: 2018 20th National power systems conference NPSC 2018, pp 1–6. https://doi.org/10.1109/NPSC.2018.8771738
36. Pahadasingh S (2021) TLBO based CC-PID-TID controller for load frequency control of multi area power system. In: 1st Odisha international conference on electrical power engineering, communication and computing technology ODICON 2021, pp 1–7. https://doi.org/10.1109/ODICON50556.2021.9429022
37. Pradhan PC, Sahu RK, Panda S (2016) Firefly algorithm optimized fuzzy PID controller for AGC of multi-area multi-source power systems with UPFC and SMES. Eng Sci Technol Int J 19(1):338–354. https://doi.org/10.1016/j.jestch.2015.08.007
38. Dash P, Saikia LC, Sinha N (2016) Flower pollination algorithm optimized PI-PD cascade controller in automatic generation control of a multi-area power system. Int J Electr Power Energy Syst 82:19–28. https://doi.org/10.1016/j.ijepes.2016.02.028
39. Siva D, Engineering E, Engineering E (2017) PSO optimized load frequency control of a multi area power system under restructured scenario. Int J Sci Technol Eng 3(07):62–68
40. Satapathy P (2018) Load frequency control with PDPID controller including double derivative filter. In: 2018 International conference on recent innovations in electrical, electronics & communication engineering, pp 240–245
41. Satapathy P (2021) PDPID plus DDF cascaded controller for LFC investigation in unified system with wind generating unit, pp 6–11. https://doi.org/10.1109/ODICON50556.2021.9428967
42. Latif A, Hussain SMS, Das DC, Ustun TS, Iqbal A (2021) A review on fractional order (FO) controllers' optimization for load frequency stabilization in power networks. Energy Rep 7(July):4009–4021. https://doi.org/10.1016/j.egyr.2021.06.088
43. Sharma D, Yadav NK (2019) Lion Algorithm with Levy Update: load frequency controlling scheme for two-area interconnected multi-source power system. Trans Inst Meas Control 41(14):4084–4099. https://doi.org/10.1177/0142331219848033
44. Jain S, Hote YV (2018) Design of fractional PID for load frequency control via Internal model control and Big bang Big crunch optimization. IFAC-PapersOnLine 51(4):610–615. https://doi.org/10.1016/j.ifacol.2018.06.163

45. Debbarma S, Saikia LC, Sinha N (2013) AGC of a multi-area thermal system under deregulated environment using a non-integer controller. Electr Power Syst Res 95:175–183. https://doi.org/10.1016/j.epsr.2012.09.008
46. Farook S, Raju PS (2012) Decentralized fractional order PID controller for AGC in a multi-area deregulated power system. Int J Adv Electr Electron Eng 1:317–332
47. Morsali J, Zare K, Tarafdar Hagh M (2018) Comparative performance evaluation of fractional order controllers in LFC of two-area diverse-unit power system with considering GDB and GRC effects. J Electr Syst Inf Technol 5(3):708–722. https://doi.org/10.1016/j.jesit.2017.05.002
48. RamBabu N, Saikia LC (2020) AGC of a multiarea system incorporating accurate HVDC and precise wind turbine systems. Int Trans Electr Energy Syst. https://doi.org/10.1002/2050-7038.12277
49. Saha A, Saikia LC (2018) Combined application of redox flow battery and DC link in restructured AGC system in the presence of WTS and DSTS in distributed generation unit. IET Gener Transm Distrib 12(9):2072–2085. https://doi.org/10.1049/iet-gtd.2017.1203
50. Saha A, Saikia LC (2019) Renewable energy source-based multiarea AGC system with integration of EV utilizing cascade controller considering time delay. Int Trans Electr Energy Syst 29(1):e2646. https://doi.org/10.1002/etep.2646
51. Latif A, Chandra Das D, Kumar Barik A, Ranjan S (2020) Illustration of demand response supported co-ordinated system performance evaluation of YSGA optimized dual stage PIFOD-(1 + PI) controller employed with wind-tidal-biodiesel based independent two-area interconnected microgrid system. IET Renew Power Gener 14(6):1074–1086. https://doi.org/10.1049/iet-rpg.2019.0940
52. Tasnin W, Saikia LC (2018) Performance comparison of several energy storage devices in deregulated AGC of a multi-area system incorporating geothermal power plant. IET Renew Power Gener 12(7):761–772. https://doi.org/10.1049/iet-rpg.2017.0582
53. Santra S, De M (2022) Comparative performance evaluation of various fractional order controllers in comparison with conventional VI controller for LFC. In: 2022 IEEE Delhi section conference, pp 1–5. https://doi.org/10.1109/DELCON54057.2022.9752865
54. Arya Y (2020) A novel CFFOPI-FOPID controller for AGC performance enhancement of single and multi-area electric power systems. ISA Trans 100:126–135. https://doi.org/10.1016/j.isatra.2019.11.025
55. Arya Y, Dahiya P, Çelik E, Sharma G, Gözde H, Nasiruddin I (2021) AGC performance amelioration in multi-area interconnected thermal and thermal-hydro-gas power systems using a novel controller Engineering Science and Technology, an International Journal AGC performance amelioration in multi-area interconnected thermal. Eng Sci Technol Int J 24(2):384–396. https://doi.org/10.1016/j.jestch.2020.08.015
56. Arya Y (2019) A new optimized fuzzy FOPI-FOPD controller for automatic generation control of electric power systems. J Franklin Inst 356(11):5611–5629. https://doi.org/10.1016/j.jfranklin.2019.02.034
57. Sekyere YOM, Effah FB, Okyere PY (2024) An enhanced particle swarm optimization algorithm via adaptive dynamic inertia weight and acceleration coefficients. J Electron Electr Eng 3(1):50–64. https://doi.org/10.37256/jeee.3120243868
58. Sekyere YOM, Effah FB, Okyere PY (2024) Optimal tuning of PID controllers for LFC in renewable energy source integrated power systems using an improved PSO. J Electron Electr Eng 3(1):65–83. https://doi.org/10.37256/jeee.3120243869
59. Arya Y, Dahiya P, Çelik E, Sharma G, Gözde H, Nasiruddin I (2021) Engineering Science and Technology, an International Journal AGC performance amelioration in multi-area interconnected thermal and thermal-hydro-gas power systems using a novel controller. Eng Sci Technol Int J 24(2):384–396. https://doi.org/10.1016/j.jestch.2020.08.015
60. Mohamed SS, Elbanna SH, Abdel-Ghany AM (2020) Fuzzy self-tuning fractional order PID controller design in load frequency control of power systems. In: 2020 12th International conference on electrical engineering ICEENG 2020, pp 89–96. https://doi.org/10.1109/ICEENG45378.2020.9171759
61. Chen H, Xiang L, Lin L, Huang S (2021) Fractional-order PID load frequency control for power systems incorporating thermostatically controlled loads. In: Proceedings of 2021 IEEE 4th international electrical energy conference CIEEC 2021, pp 3–8. https://doi.org/10.1109/CIEEC50170.2021.9510621
62. Kennedy J, Eberhart R (1995) Particle swarm optimization. In: Proceedings of ICNN'95—international conference on neural networks, IEEE, pp 1942–1948. https://doi.org/10.1109/ICNN.1995.488968
63. Twumasi E, Frimpong EA, Kwegyir D, Folitse D (2021) Improvement of grey system model using particle swarm optimization. J Electr Syst Inf Technol. https://doi.org/10.1186/s43067-021-00036-9
64. Sahu RK, Panda S, Padhan S (2015) A hybrid firefly algorithm and pattern search technique for automatic generation control of multi area power systems. Int J Electr Power Energy Syst 64:9–23. https://doi.org/10.1016/j.ijepes.2014.07.013
65. Babu NR, Chandra Saikia L, Bhagat SK, Kumar Ramoji S, Dekaraja B, Behera MK (2020) Optimal location of AC-HVDC tie-line in a multi-area LFC system incorporated with renewable and ESD considering CA optimized PI-TID cascade controller. In: 2020 IEEE 17th India council international conference INDICON 2020. https://doi.org/10.1109/INDICON49873.2020.9342506
66. Rasolomampionona D, Klos M, Cirit C, Montegiglio P, De Tuglie EE (2022) A new method for optimization of Load Frequency Control parameters in multi-area power systems using genetic algorithms. In: 2022 IEEE international conference on environment and electrical engineering and 2022 IEEE industrial and commercial power systems Europe. EEEIC/I CPS Europe 2022. https://doi.org/10.1109/EEEIC/ICPSEurope54979.2022.9854535
67. Ranjan M, Shankar R, Saxena A, Rai P (2022) Design and analysis of novel QOAOA optimized type-2 fuzzy FOPIDN controller for AGC of multi-area power system. In: 2022 2nd International conference on emerging frontiers in electrical and electronic technologies ICEFEET 2022, pp 1–6. https://doi.org/10.1109/ICEFEET51821.2022.9847973
68. Jaber HH, Miry AH, Al-Anbarri K (2022) Load frequency control of interconnected power system using artificial intelligent techniques based fractional order PIλDμcontroller. AIP Conf Proc 2386(December):2–7. https://doi.org/10.1063/5.0066839
69. Liu M, Bizzarri F, Brambilla AM, Milano F (2019) On the impact of the dead-band of power system stabilizers and frequency regulation on power system stability. IEEE Trans Power Syst 34(5):3977–3979. https://doi.org/10.1109/TPWRS.2019.2920522

70. Bryant JS, Sokolowski P, Meegahapola L (2020) Influence of governor deadbands on power grids with high renewable penetration. In: Proceedings of 2020 international conference on smart grids and energy systems SGES 2020, pp 685–690. https://doi.org/10.1109/SGES51519.2020.00127

Publisher's Note

Springer Nature remains neutral with regard to jurisdictional claims in published maps and institutional affiliations.